Studies of Adenosine Triphosphatase Activity and Turbidity in Myofibril and Actomyosin Suspensions*

David R. Kominz

ABSTRACT: Steady-state adenosine triphosphatase (ATPase) determinations at low adenosine triphosphate (ATP) concentrations were performed in the pH-Stat utilizing acetyl phosphate and *Escherichia coli* acetokinase as ATP-regenerating system. This permitted simultaneous measurement of ATPase activity and turbidity at 10^{-5}–10^{-3} M ATP. It was confirmed that in addition to binding to the hydrolytic site, ATP also binds to a clearing site in actomyosin and myofibrils. Following binding of ATP to the clearing site, removal of bound ATP or readdition of Ca^{2+} caused the development of heightened turbidity, suggesting that a conformational change had resulted from the ATP binding at the clearing site. The apparent binding constant to the clearing site and the apparent V_{max} of the actomyosin ATPase were both sensitive to traces of Ca^{2+} in the presence of native tropomyosin. Coupling between this binding and ATPase activation is suggested by their parallel ionic strength and temperature dependence and by the reciprocal changes in ΔH of binding and $\Delta H^{\ddagger}$ of activation with temperature. Computations support a model based on cooperative and competitive binding. A cyclic ATPase is proposed, which couples ATPase activity to reversible actin binding through an interaction and exchange of ATP bound at the clearing site with ATP bound and split at the hydrolytic site.

The existence of a second regulatory binding site for ATP on myosin, in addition to the site of ATP hydrolysis, has been proposed by a number of workers (Nihei and Tonomura, 1959; Levy and Fleisher, 1965; Eisenberg and Moos, 1965; Kominz, 1965, 1966; Kiely and Martonosi, 1968). Levy and Fleisher (1965) stated explicitly that "the concerted action of two or more molecules of ATP (ITP) operating simultaneously or sequentially at two or more sites in the protein complex" is involved in superprecipitation. The binding of a second ATP may prevent (Kominz, 1965) or accelerate (Kominz, 1966) conformational change affecting the enzymatic site. Kiely and Martonosi (1968) propose that the triphosphate chain of a single ATP molecule may bind to either the hydrolytic or the regulatory area.

It is well known that ATP and pyrophosphate can cause dissociation of actin from myosin (Weber and Portzehl, 1952) or from H-meromyosin (Perry *et al.*, 1963; Yagi *et al.*, 1965). ATP also causes configurational changes in the myosin or H-meromyosin which contribute to the hydrodynamic and turbidity changes (Blum and Morales, 1953). Morita (1967, 1969) has found a configurational change associated with the hydrolytic site which temporarily buries some tyrosyl and tryptophyl chromophores. At low ionic strength, the same processes are involved in the immediate clearing or turbidity development which occurs when ATP is added to an actomyosin or myofibril suspension (Maruyama and Gergely, 1962). In the presence of the native tropomyosin regulatory system (Ebashi and Ebashi, 1964; Ebashi and Endo, 1968), reducing free Ca^{2+} below 10^{-6} M by means of EGTA[1] allows clearing to occur at very low ATP concentrations (Kominz and Yoshioka, 1969).

In our earlier work, it was not possible to examine ATPase activities at low ATP concentrations (Kominz and Yoshioka, 1969). In the present paper, a new technique of ATPase measurement has allowed simultaneous recording of turbidity changes and ATPase activity at all ATP concentrations. An indicator dye can effectively follow rapid transients (Tokiwa and Tonomura, 1965; Finlayson and Taylor, 1969), but not steady-state kinetics, at low ATP concentration. The pH-Stat has not previously been used at low ATP concentration because the usual regenerating systems, creatine kinase and pyruvate kinase, do not liberate a proton. With acetokinase as the regenerating system, it has been possible to measure simultaneously turbidity and steady-state ATPase activity at very low ATP concentration.

Materials and Methods

Myofibrils were prepared by homogenizing minced fresh rabbit psoas muscle for 4 min in ten volumes of 0.02 M KCl–0.008 M Tris-maleate (pH 6.85) buffer containing 0.004 M EDTA. The suspension was filtered through cheesecloth and centrifuged gently at 650*g* for 20 min at 5°. The supernatant was discarded, and the precipitate was resuspended in the same solution and centrifuged twice more. A concentrated suspension of the myofibrils was slowly diluted with ice-cold glycerol to 50% and stored in the deep freeze at −20°. For measurements of ATPase and turbidity, 0.5 ml of a 1-month-old 6-mg/ml suspension was added to a reaction volume of 20 ml. The reaction mixture then contained 1.25% glycerol and 5×10^{-5} M EDTA. This small amount of glycerol has been found to be without significant effect upon turbidity (Maruyama and Kominz, 1969) or ATPase activity (Kominz, 1966). Calculation of Mg^{2+} distribution took account of the EDTA present.

* From the National Institute of Arthritis and Metabolic Diseases, National Institutes of Health, Public Health Service, U. S. Department of Health, Education, and Welfare, Bethesda, Maryland 20014. *Received November 3, 1969.*

[1] Abbreviations used are: EGTA, ethylene glycol bis(β-aminoethyl ether)-*N,N'*-tetraacetic acid; pATP, negative logarithm of ATP concentration; pCa, negative logarithm of Ca^{2+} concentration.

Actomyosin was prepared by the method of Stowring *et al.* (1966). It was stored in the refrigerator at 0° until examined. Acetokinase from *Escherichia coli* was obtained from Boehringer Mannheim as a 5-mg/ml suspension in 2.4 M $(NH_4)_2SO_4$, containing approximately 80 units of activity/mg. ATP and acetyl phosphate were reagent grade chemicals; 0.1 M stock solutions at pH 7.5 were stored frozen until use.

ATPase activity and turbidity were examined simultaneously in the apparatus described by Evans and Bowen (1968). Modifications allowing for temperature monitoring and control were installed during the course of this work. Because the phototube output yields per cent transmission, % T, optical densities were calculated.

The usage in this paper, following that of Saroff (1966) and London and Steck (1969), has been to employ association constants, denoting them by $K_{\text{subscript}}$. If the use of a dissociation constant was necessary, a small superscript d has been employed, as in pK^d. Calculation of $MgATP^{2-}$ and free Mg^{2+} employed a value of 3.8×10^4 for K_{MgATP}, and calculations of free Ca^{2+} employed a value of 8×10^3 for K_{CaATP} (Sillen and Martell, 1964).

Although the acetokinase $K_m{}^d$ values of 5×10^{-3} M for Mg^{2+} and acetyl phosphate (Rose, 1962) are similar to those of creatine kinase for Mg^{2+} and creatine phosphate (Kuby and Noltmann, 1962), the acetokinase $K_m{}^d$ of 1.5×10^{-3} M for ADP is about ten times higher than that of creatine kinase. This implies that tenfold more ADP will be present in the steady state with acetokinase than with creatine kinase, under otherwise comparable conditions. Measurements of steady-state ATPase values were made at pH 7.5, generally in the presence of 1.5 mM acetyl phosphate, 0.05 mg of acetokinase, and 0.5 mM Mg^{2+}; zero-order kinetics were obtained at all reaction rates studied. The reaction rate of 0.05 mg of acetokinase was 80% of the extrapolated value for infinite acetokinase concentration, when examined at pATP 4.7. This means that above pATP 4.5 the steady-state ATPase activity will be measured at ATP concentrations slightly less than the initial one, and it could be expected that artificial flattening of a plot of ATPase activity against pATP will occur as the pATP is extended beyond 5. Turbidity values were the same whether acetokinase or creatine kinase were employed as regenerating system. A small steady rate of alkali uptake occurred prior to the addition of ATP, presumably due to actomyosin-bound ADP. Tests of myofibril preparations for acetyl phosphohydrolase (Lipmann and Tuttle, 1945) were negative. In the one case where Mg^{2+} was allowed to become limiting (Figure 2, curve 3), this was set at sufficiently high ATP concentration so that if the acetokinase were inhibited, a shift from net acetyl phosphate hydrolysis to ATP hydrolysis could occur.

Two methods of measuring ATPase activity and turbidity were employed. In the method of gradual ATP addition, ATP was added at a very low level, and steady-state ATPase and turbidity values were measured; ATP was then added to achieve a slightly higher concentration, and the process was repeated. In this way, precise comparison of ATPase and turbidity values could be made on the same sample at 10^{-5}–10^{-3} M ATP. The second method is essentially that of Matsunaga and Noda (1966), as modified by Kominz and Yoshioka (1969). A myofibril or actomyosin suspension was brought immediately to an intermediate ATP concentration, and the steady-state values of turbidity and ATPase activity

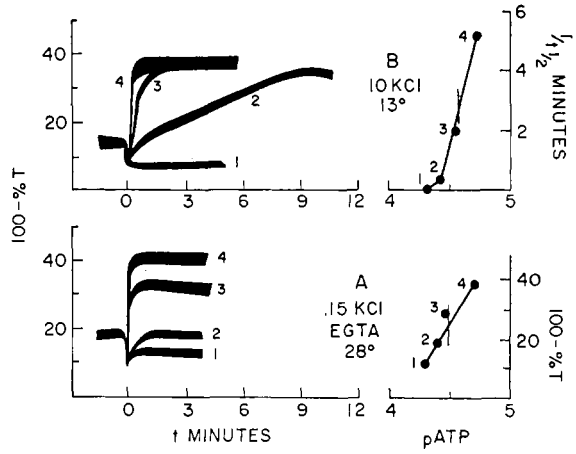

FIGURE 1: Method of estimation of $pATP_{50}$ above and below 18°. Left: turbidity development in actomyosin suspensions; right; graphic estimation of $pATP_{50}$. The 20-ml reaction mixture contained 10 mg of actomyosin, 1.0 mM acetyl phosphate, 0.05 mg of acetokinase, and 5×10^{-4} M Mg^{2+} at pH 7.5. (A) 28°, 0.15 M KCl, 1×10^{-5} M EGTA, and the following concentrations of ATP: (1) 5×10^{-5} M, (2) 4×10^{-5} M, (3) 3×10^{-5} M, and (4) 2×10^{-5} M. (B) 13°, 0.10 M KCl and the following concentrations of ATP: (1) 5×10^{-5} M, (2) 4×10^{-5} M, (3) 3.5×10^{-5} M, and (4) 2×10^{-5} M.

were examined either in the absence of EGTA or first in the presence of excess EGTA and then of added Ca^{2+}.

The midpoint of turbidity development will be called $pATP_{50(EGTA)}$ if obtained in the presence of excess EGTA, and $pATP_{50(Ca^{2+})}$ if obtained in the presence of traces of free Ca^{2+}. At temperatures above 18°, steady-state turbidity values are rapidly attained, as seen in Figure 1A, left; the value of pATP at 50% turbidity development is obtained by graphic estimation (Figure 1A, right). At temperatures below 18°, turbidity development appears to be an all-or-none phenomenon, so that the transition zone involves a kinetic rather than a steady-state process (Figure 1B, left); for these temperatures, values of $pATP_{50}$ have been estimated from plots of reciprocal half-times of turbidity development (Figure 1B, right).

Results

Myofibril ATPase Activity and Turbidity. Figure 2 plots the ATPase activity of a myofibril suspension to which increments of ATP were added under four sets of conditions. Sample 3 was Mg^{2+} limited; ATP was added to samples 1 and 2 in the form of $MgATP^{2-}$. EGTA bound Ca^{2+} in sample 2; an excess of Ca^{2+} was present in sample 4. The course of each experiment commences with the initial ATP addition in the lower right-hand corner of Figure 2 and proceeds through increasing ATP concentrations (decreasing pATP values) toward the left.

There was a parallel development of ATPase activity in samples 1 and 2 until pATP 5; with further ATP addition, the two curves sharply diverged. This confirms the recent results of Weber (1969), in which creatine kinase was employed as regenerating system. In the presence of traces of Ca^{2+}, the hydrolytic rate increased markedly until pATP 3.5; in the presence of EGTA, the rate started to rise but returned

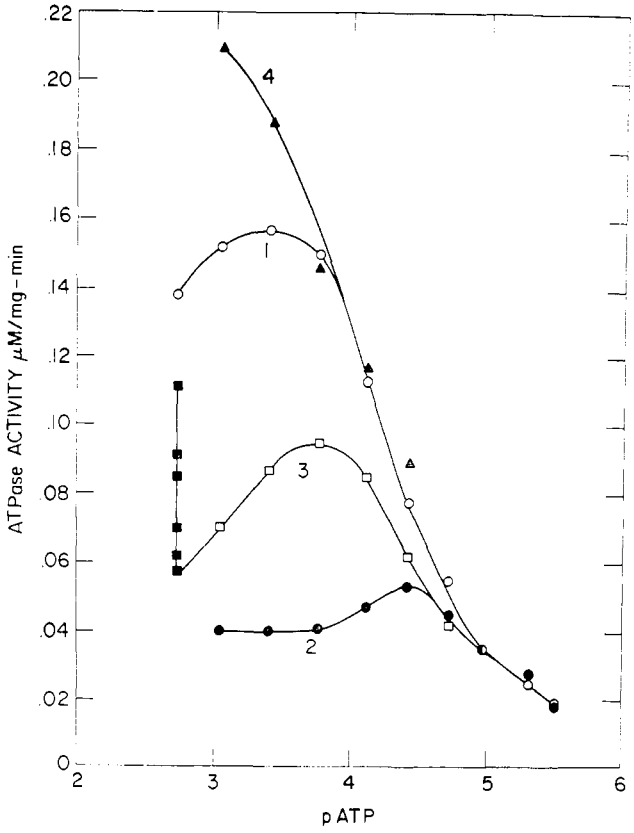

FIGURE 2: Dependence of myofibrillar ATPase activity on substrate concentration at 0.14 M KCl. The 20-ml reaction mixture contained 3 mg of myofibrils, 1.5 mM acetyl phosphate, and 0.05 mg of acetokinase at pH 7.5 and 27–30°. To each of four samples, increments of ATP or $MgATP^{2-}$ were added serially; the time course of each experiment proceeds from lower right to upper left. (○) Sample 1, no EGTA, 4.5×10^{-4} M Mg^{2+}, additions of $MgATP^{2-}$; (●) sample 2, 5×10^{-5} M EGTA, 4.5×10^{-4} M Mg^{2+}, additions of $MgATP^{2-}$; (□) sample 3, no EGTA, 0.75×10^{-4} M Mg^{2+}, additions of ATP; (■) after the ATP concentration in sample 3 was brought to 1.9×10^{-3} M, the Mg^{2+} concentration was raised in serial increments to 3×10^{-3} M; (▲) sample 4, 2.5×10^{-5} M Ca^{2+}, 4.5×10^{-4} M Mg^{2+}, additions of ATP.

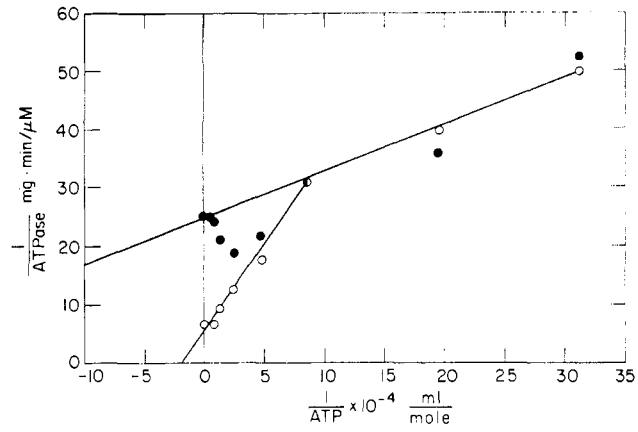

FIGURE 3: Lineweaver–Burk plot of myofibrillar ATPase activity at 0.14 M KCl. Data from samples 1 and 2 of Figure 2 have been replotted; symbols are the same as in Figure 2.

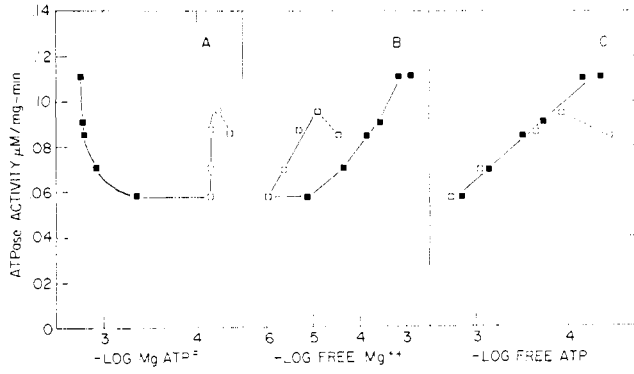

FIGURE 4: Dependence of myofibrillar substrate inhibition on (A) $MgATP^{2-}$, (B) free Mg^{2+}, (C) free ATP concentrations. Data are calculated for sample 3 of Figure 2; symbols are the same as in Figure 2.

quickly to the basal level. In Figure 3, double-reciprocal plots allow tentative calculation of V_{max} and pK^d for the basal and activated processes. The basal ATPase appears to have a V_{max} of 0.04 μmole/mg min and pK_I^d of 5.5. For the activated ATPase, curve 1 suggests a V_{max} of 0.18 μmole/mg min and a pK_{II}^d of 4.25. However these values have been affected by the slight substrate inhibition of curve 1; the values obtainable in the presence of added Ca^{2+} from curve 4 are a V_{max} of 0.22 μmole/mg min and a pK_{II}^d of 4.21.

Sample 3 of Figure 2 contained traces of Ca^{2+} and was Mg^{2+} limited. There was substrate inhibition at 0.1–1.9 mM ATP (pATP 4–2.7). At pATP 2.7 stepwise addition of Mg^{2+} gradually released the substrate inhibition and allowed the ATPase activity to approach that of the control. The concentration of $MgATP^{2-}$, free Mg^{2+} and free ATP were calculated for this sample over the range of substrate inhibition at 0.8×10^{-4} M Mg^{2+}, and over the range of $0.8–25.0 \times 10^{-4}$ M Mg^{2+} at pATP 2.7. There is no correlation between ATPase activity and $MgATP^{2-}$, as seen in Figure 4A. There is a correlation between ATPase activity and free Mg^{2+} in Figure 4B; however the hysteresis would suggest the unusual situation of a site being less available to Mg^{2+} binding than to release. The only correlation that is linear and reversible is between ATPase activity and free ATP in Figure 4C.

To a duplicate of sample 3, instead of multiple additions of Mg^{2+}, a single addition of 2.5×10^{-5} M Ca^{2+} was made at pATP 2.7. This restored the ATPase activity from 0.05 to 0.16 μmole per mg min. Since the free ATP remained virtually unchanged, this suggests that the role of free ATP in causing substrate inhibition might be related to its action on bound Ca^{2+} (Perry and Grey, 1956; Weber, 1959). It could effect the release of this bound Ca^{2+} through a competitive binding process, through complex formation, or both.

At very low ATP concentrations, all of the samples of Figure 2 developed turbidity which reached a maximum at pATP 5.0 as shown in Figure 5. Further addition of ATP lowered the turbidity again; the pATP dependence of the turbidity reversal was steeper in the presence of EGTA than in its absence. In both cases reversal of turbidity was incomplete, and it required a much broader range of pATP than was required to define the clearing zone (Figure 5, dashed

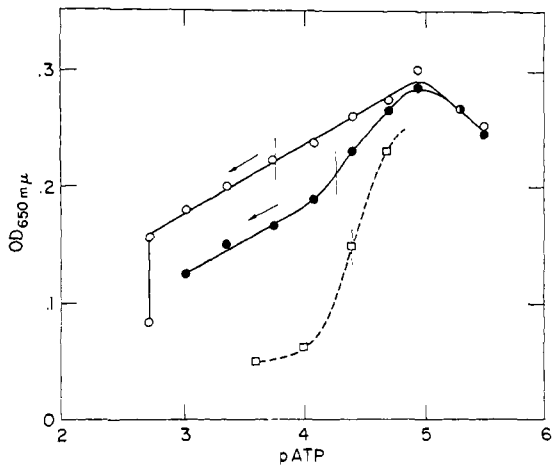

FIGURE 5: Dependence of myofibrillar turbidity development and reversal on substrate concentration at 0.14 M KCl. (○ and ●) Turbidity values which accompanied the ATPase activities of samples 1 and 2, Figure 2; symbols are the same as in Figure 2. At 1.9×10^{-3} M ATP, sample 1 was brought to 5×10^{-5} M EGTA. (□) Four separate samples without EGTA containing 4.5×10^{-4} M Mg^{2+}. Vertical bars suggest pATP of 50% turbidity development or reversal.

line). Some actomyosin samples had a similar broad range of turbidity reversal, but generally reversal could be accomplished over a range of 1 pATP unit.

If the ATPase activities of Figure 2 are plotted against the turbidity values of the same samples in Figure 5, the roughly triangular relationship of Figure 6 is obtained. The base of the triangle is given by sample 2 containing EGTA, whose basal level of ATPase activity is almost independent of the state of clearing. The right side of the triangle indicates a linear relationship between ATPase activation and the development of clearing; it resembles the systems studied by Perry *et al.* (1963) because presumed dissociation of actomyosin is accompanied by heightened ATPase activity. The left side of the triangle represents substrate inhibition; it is displaced to the right as in samples 2 and 3 when the free Ca^{2+} is reduced. Similar triangular relationships are obtained when actomyosin suspensions are examined. The addition of excess Ca^{2+} to an EGTA sample brings it from a clear state of low ATPase activity to a position along the fully activated right-hand side of the triangle, as illustrated by lines a and b.

Actomyosin Turbidity and ATPase Activity. Values of $pATP_{50}$ obtained as in Figure 1A with actomyosin suspensions at 0.05, 0.10, and 0.15 ionic strength at 22–24° are listed in Table I. At each ionic strength chelation of Ca^{2+} with excess EGTA causes a shift of about 0.8 from $pATP_{50(Ca^{2+})}$ to $pATP_{50(EGTA)}$. For a change of 0.1 in ionic strength, there is a change of about 1.0 in the $pATP_{50}$.

The turbidities observed as in Figure 1 are never very high, and the maximum in the presence of traces of Ca^{2+} is not much greater than that in the presence of excess EGTA. However if increasing amounts of Ca^{2+} are added to a sample initially containing EGTA, quite high levels of turbidity may be attained. Figure 7B portrays the experimental result of adding Ca^{2+} at five different ATP concentrations. In Figure 7A, the same data are replotted in terms of adding ATP to four different Ca^{2+} concentrations.

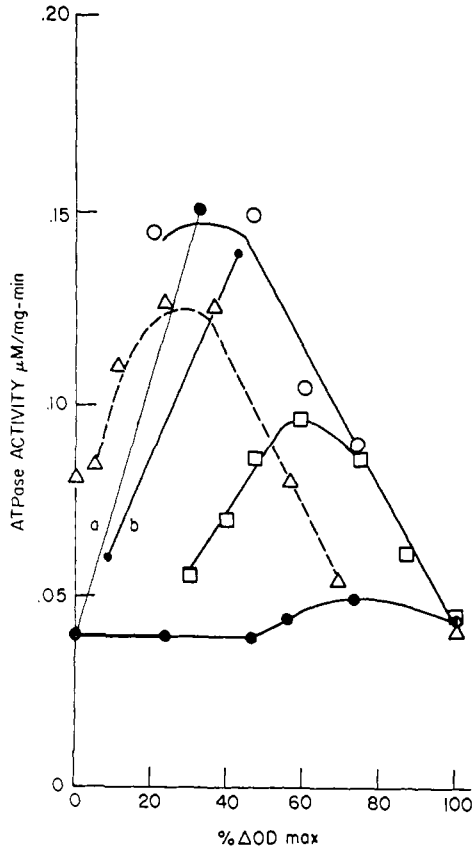

FIGURE 6: Relation between myofibrillar ATPase activity and turbidity. (○) Sample 1 of Figures 2 and 5; (●) sample 2 of Figures 2 and 5; (□) sample 3 of Figure 2; (△) 4.8 mg of myofibrils, 0.05 M KCl, 5×10^{-5} M EGTA, 4.5×10^{-4} M Mg^{2+}, additions of ATP. The effect of adding excess Ca^{2+} to cleared myofibril suspensions: (a) sample 2 of Figures 2 and 5, 7.5×10^{-5} M Ca^{2+} added at 1×10^{-3} M ATP. (b) 3.2 mg of myofibrils, 0.05 M KCl, 5×10^{-5} M EGTA, and 4.5×10^{-4} M Mg^{2+}; 5×10^{-5} M Ca^{2+} added at 2.5×10^{-4} M ATP.

TABLE I: ATP Requirement for Clearing in the Presence or Absence of EGTA at Various Ionic Strengths.[a]

Γ/2	$pATP_{50(EGTA)}$	$pATP_{50(Ca^{2+})}$
0.05	3.95	3.25
0.10	4.55	3.75
0.15	5.0	4.25

[a] Estimations were performed as in Figure 1A at 22–24°.

Substituting turbidity for enzymatic activity as ordinate, there is a strong resemblance between these plots and those of London and Steck's (1969) model III in which both activating metal and metal–substrate complex bind independently to the enzyme. The ATP activates and then inhibits as its concentration is raised. As the concentration of metal is raised, a constant level of turbidity is found at low fixed ATP, and a steep climb in turbidity is found at higher fixed ATP; not present in the model however is an upper limit of

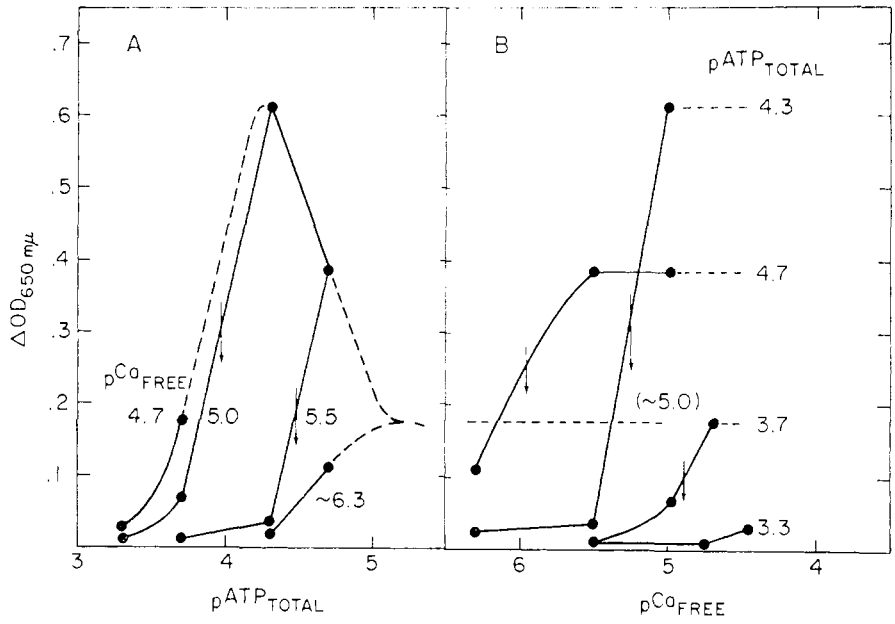

FIGURE 7: Dependence of actomyosin turbidity development on free Ca^{2+} and total ATP concentration. The 20-ml reaction mixture contained 10 mg of actomyosin, 1.0 mM acetyl phosphate, 0.05 mg of acetokinase, 0.10 M KCl, 1×10^{-5} M EGTA, and 5×10^{-4} M Mg^{2+} at pH 7.5 and 22–24°. The experiments were performed by adding increments of 1×10^{-5} M Ca^{2+} to suspensions held at constant ATP concentration, as shown in part B. The data are replotted as variable ATP at constant free Ca^{2+} in part A; the dashed lines extend the boundaries into the region of basal turbidity at low ATP and into the region of clearing in the presence of excess Ca^{2+} at high ATP. Arrows denote the $pATP_{50}$ at constant Ca_{FREE} in part A, and the $pCa_{FREE-50}$ at constant ATP in part B.

ATP concentration above which no addition of Ca^{2+} can cause a turbidity increase. This limit is denoted by the dashed line at the left of Figure 7A.

The native tropomyosin system operates within the region of Figure 7A enclosed by the dashed lines. It allows clearing to occur at low ATP concentrations with a Hill *n* (Loftfield and Eigner, 1969) of 1 if the free Ca^{2+} is low enough (here estimated as about pCa 6.3). At higher levels of free Ca^{2+}, it allows clearing to occur with a Hill *n* of 2.5–3; the same *n* is obtained for turbidity development on adding Ca^{2+} to cleared samples in Figure 7A. At high levels of free Ca^{2+} or when native tropomyosin is absent, clearing occurs with a Hill *n* of 2.5–3, but no turbidity develops on adding Ca^{2+} to cleared samples.

Two values of $pATP_{50}$ obtained at constant pCa in Figure 7A are plotted as open circles in Figure 8, and three values

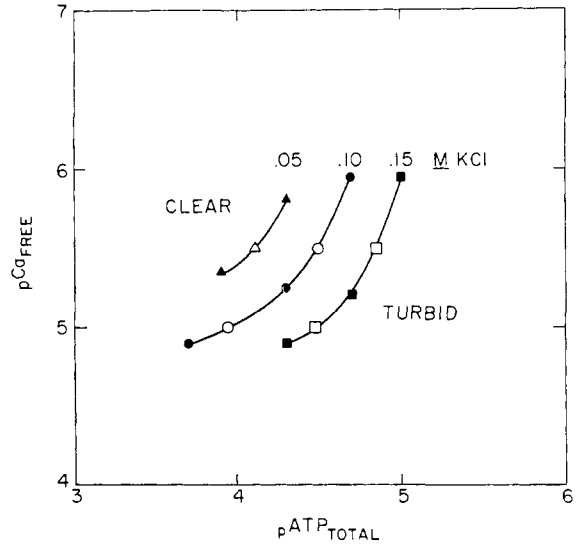

FIGURE 8: The dependence of 50% turbidity development on free Ca^{2+} and total ATP concentration at three ionic strengths. The 50% turbidity points were obtained as in Figure 7; closed symbols are $pCa_{FREE-50}$ at constant ATP; open symbols are $pATP_{50}$ at constant Ca_{FREE}. (△, ▲) 0.05 M KCl, (○, ●) 0.10 M KCl, and (□, ■) 0.15 M KCl.

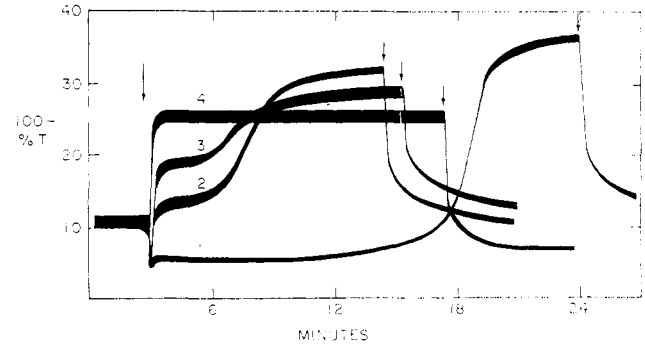

FIGURE 9: The relation between the initial development of turbidity in actomyosin suspensions upon addition of ATP, and the final increase in turbidity upon exhaustion of ATP. The 20-ml reaction mixture contained 10 mg of actomyosin in 0.10 M KCl, 5×10^{-4} M Mg^{2+} at pH 7.5 and 21–22°. Initial ATP concentrations were: (1) 1×10^{-4} M, (2) 5×10^{-5} M, (3) 4×10^{-5} M, and (4) 2×10^{-5} M. Reversal of turbidity was obtained by adding 5×10^{-5} M EGTA and then raising the ATP to 1–2.5 $\times 10^{-4}$ M. Arrows denote additions of ATP.

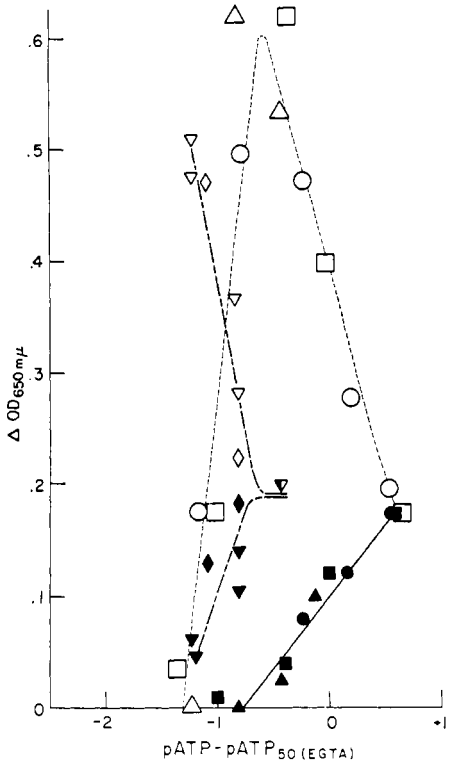

FIGURE 10: Turbidity development in the presence or absence of an ATP-regenerating system. Abscissa represents pATP normalized to $pATP_{50(EGTA)}$ = 0. The 20-ml reaction mixture contained 10 mg of actomyosin, 5 × 10^{-5} M Mg^{2+} at pH 7.5 and 22–24°. In the presence of 1.0 mM acetyl phosphate and 0.05 mg of acetokinase, closed symbols represent the turbidity in the presence of 10^{-5} M EGTA, open symbols represent the turbidity in the presence of 2 × 10^{-5} M Ca^{2+}: (▲,△) 0.15 M KCl, $pATP_{50(EGTA)}$ = 5.0; (■,□) 0.10 M KCl, $pATP_{50(EGTA)}$ = 4.55 (see Figure 7); (●,○) 0.05 M KCl, $pATP_{50(EGTA)}$ = 3.95. In the absence of regenerating system, pATP refers to the initial ATP concentration, closed symbols represent the initial turbidity plateau, open symbols represent the final turbidity values: (▼,▽) 0.15 M KCl, $pATP_{50}$ = 5.0; (◆,◊) 0.10 M KCl, $pATP_{50}$ = 4.55.

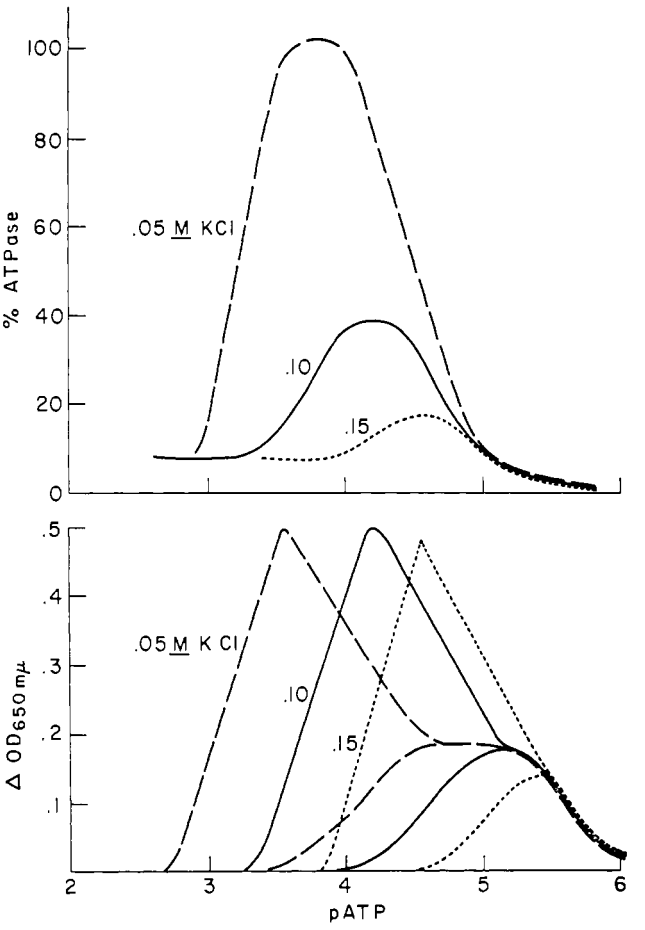

FIGURE 11: Comparison of pATP dependence of ATPase activity to that of turbidity. Bottom: data of Figure 10 have been plotted at original pATP values. Top: to 20-ml reaction mixture containing 8–10 mg of actomyosin, 1.0 mM acetyl phosphate, 0.05 mg of acetokinase, 5 × 10^{-5} M EGTA, and 5 × 10^{-4} M Mg^{2+} at pH 7.5 and 21–22°, gradually increasing increments of ATP were added. (· · · · ·) 0.15 M KCl, (——) 0.10 M KCl, and (- - - -) 0.05 M KCl.

of pCa_{50} obtained at constant pATP in Figure 7B are plotted as closed circles in Figure 8. All five points fall on the same curve, which defines the operating zone of the native tropomyosin system at 0.1 M KCl. A similar zone has been defined for 0.15 M KCl, and a partial zone for 0.05 M KCl. Figure 8 indicates that an increase in ionic strength would have the following effect on clearing: at fixed Ca^{2+}, less ATP would be required to produce clearing; at fixed ATP, more Ca would be required to maintain the bound Ca^{2+} at the level corresponding to 50% turbidity. Competitive K^+ binding would explain the increased Ca^{2+} requirement at constant pATP; however since it also competes with H^+ binding, it would produce an increased requirement for ATP at constant pCa. An electrostatic interaction, which would have the opposite effect on anions as on cations, could explain both the Ca^{2+} and the ATP changes.

If the regenerating system was omitted to allow rapid exhaustion of substrate, a plateau turbidity value persisted until the ATP was nearly gone, when a secondary rise in turbidity occurred (Figure 9). Lower plateau values resulted in higher final values of turbidity. The final turbidity could be reversed by readdition of ATP; if EGTA was added prior to ATP, nearly complete reversibility was attainable. The cycle could be repeated several times.

The results of such turbidity studies at two ionic strengths are superimposed in Figure 10. The curves for clearing in the presence of EGTA, with the $pATP_{50(EGTA)}$ values normalized at 0, are located in the lower right. Approximately one pATP unit to the left is located the curve for clearing in the presence of Ca^{2+}. Matching each point on this clearing curve and plotted directly above it is a point representing the final turbidity value of that sample. At the right of this figure are plotted values of maximum turbidity obtained as in Figure 7B when Ca^{2+} is added following clearing in the presence of EGTA. In both cases clearing is required for the development of increased turbidity, and an inverse proportionality is observed between the degree of initial clearing and the degree of extra turbidity.

The effects of ionic strength on the pATP dependence of turbidity development and on the pATP dependence of ATPase activity are compared in Figure 11. The effect of decreasing ionic strength on turbidity is to shift the entire

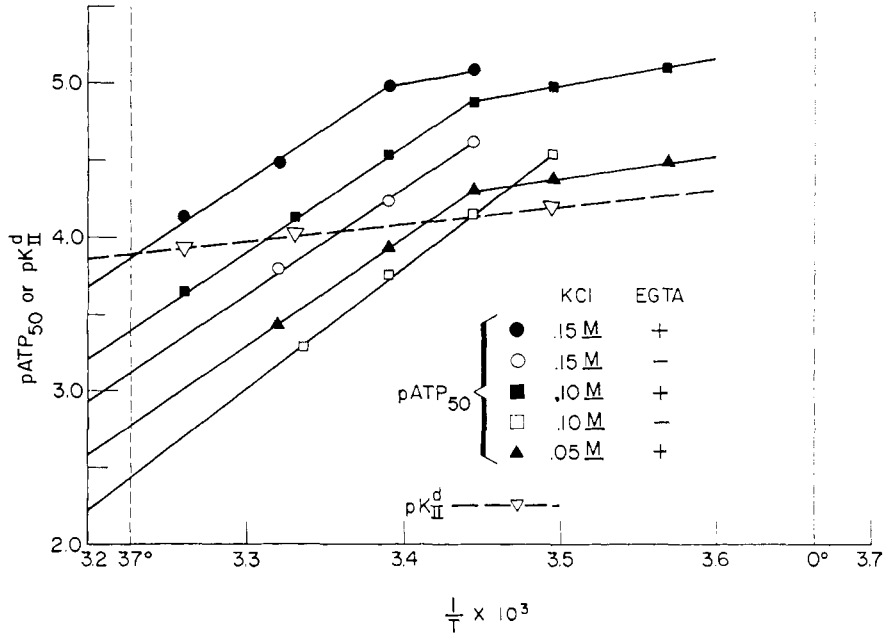

FIGURE 12: Temperature dependence of actomyosin turbidity and ATPase activity. The 20-ml reaction mixture contained 10 mg of actomyosin, 1.0 mM acetyl phosphate, 0.05 mg of acetokinase, and 5×10^{-4} M Mg^{2+} at pH 7.5. In the case of $pATP_{50}$ values, closed symbols represent the $pATP_{50(EGTA)}$ in the presence of 1×10^{-5} M EGTA, open symbols represent the $pATP_{50(Ca^{2+})}$ in the absence of EGTA: (●,○) 0.15 M KCl, (■,□) 0.10 M KCl, and (▲) 0.05 M KCl. (- -▽- -) Ionic strength independent pK^{d}_{II} of ATPase activity, obtained as in Figure 3.

TABLE II: Thermodynamic Parameters Derived from Figure 12.

$pATP_{50}$	$\Gamma/2$	Temp (°C)	ΔH (kcal)	$\Delta F_{22°}$ (kcal)	ΔS (eu)
(Ca^{2+})	0.15	>18	−30.6	−5.7	−84
(Ca^{2+})	0.10	>18	−36.5	−5.0	−107
(EGTA)	0.15	>18	−31.0	−6.7	−82
(EGTA)	0.10	>18	−31.5	−6.1	−86
(EGTA)	0.05	>18	−32.0	−5.3	−90
				$\Delta F_{17°}$	
(EGTA)	0.10	<18	−8.7	−6.5	−7.6
(EGTA)	0.05	<18	−7.5	−5.6	−6.4
$pK_{II}{}^{d}$	0.05–0.15	13–33	−7.3	−5.6	−5.9

clearing curve to lower pATP values with no change in amplitude; the complete superimposability of the three clearing curves has been demonstrated in Figure 10. The effect of decreasing ionic strength on ATPase is not to shift the ATPase activation curve but to displace to lower pATP values the onset of substrate inhibition. The parameters clearly altered by ionic strength variation are thus the $pATP_{50}$ of the clearing process and the apparent V_{max} of the ATPase.

The effect of temperature on these parameters was next examined. From a plot of log V_{max} *vs.* $1/T$, the heat of activation was calculated to be 12–15 kcal, in agreement with Levy *et al.* (1959). For turbidity measurements at temperatures below 18°, the reciprocal half-times of turbidity development were used to obtain $pATP_{50}$ as illustrated in Figure 1B. Values of $pATP_{50(EGTA)}$ at three ionic strengths and of $pATP_{50(Ca^{2+})}$ at two ionic strengths are plotted against $1/T$ in Figure 12. Thermodynamic functions derived from the plots are listed in Table II. A large negative enthalpy of about −30 kcal and large negative entropy of about −90 eu are associated with clearing above 18°. Below 18° clearing in the presence of EGTA has a small negative enthalpy of about −8 kcal and negative entropy of about −7 eu, similar to the values found for ATP binding to the hydrolytic site in the case of $pK_{II}{}^{d}$. The clearing reaction is most efficient at low temperatures, while at higher temperatures because of the large opposing entropy term higher ATP concentrations are required to drive it.

Discussions

Role of ATP Binding. Both the development of ATPase activity and the clearing in the presence of EGTA have a Hill *n* (Loftfield and Eigner, 1969) of 1. Each of these two processes must result from the interaction of ATP at two

distinct sites; this is indicated because the $pATP_{50(EGTA)}$ is dependent on ionic strength while the $pK_{II}{}^{d}$ is not, and because the temperature dependence of these two parameters is different (Figure 12). Since there are two ATPase sites on each molecule of myosin (Slayter and Lowey, 1967), the unit to which the Hill n applies will presumably be the half-molecule for the ATPase site and also for the clearing site. In the case of the $pATP_{50(EGTA)}$, since EGTA has already sequestered and removed bound Ca^{2+}, the ATP interaction must be by binding to the protein at the clearing site.

At higher levels of Ca^{2+}, the Hill n suggests that 2.5–3 moles of ATP must interact to produce clearing. Within the zone of native tropomyosin regulation, free ATP complexes with Ca^{2+}, removing bound Ca^{2+} from troponin. By reducing the interaction between actin and myosin, this may operate in a cooperative manner to facilitate binding of a second ATP to the clearing site.

A good approximation to the experimental clearing curves with their dependence of Hill n on pATP was obtained with eq 1, the model for cooperative and competitive binding.

$$\begin{array}{ccccc} M^0 + H^+ & \overset{K_H}{\rightleftharpoons} & M + S & \overset{K_S}{\rightleftharpoons} & M^S \\ + & & + & & + \\ A & & A & & A \\ \Big\downarrow\Big\uparrow K_A & & \Big\downarrow\Big\uparrow K_A & & \Big\downarrow\Big\uparrow K_{A'} \\ AM^0 + H^+ & \overset{K_H}{\rightleftharpoons} & AM + S & \overset{K_{S'}}{\rightleftharpoons} & AM^S \end{array} \qquad (1)$$

Here A is actin, M is myosin, and S is ATP. M^0 refers to the clearing site; M^S represents a conformational change of myosin in the presence of ATP bound to the clearing site. K_A is the unperturbed binding constant of actin to myosin; K_A' is the reduced binding constant when ATP is bound at the clearing site; K_S is the binding constant of ATP to the clearing site; K_S' is the reduced binding constant in the presence of bound actin; $K_A/K_A' = K_S/K_S'$. There is a close analogy to the mutual antagonism between actin and pyrophosphate binding found by Kiely and Martonosi (1968). The regulatory effect of native tropomyosin can be expressed through these constants: as Ca^{2+} binds to troponin, the binding constant for actin increases from K_A' to K_A and the binding constant for ATP decreases from K_S to K_S'.

A computer program was utilized, employing appropriate values for binding constants and total concentration of reactants. The experimental ionic strength dependence of clearing could be reproduced only if the binding constants were multiplied by an electrostatic term in which the radius of the protein was 15–20 Å, corresponding to a molecular weight of 10,000–20,000. This strongly suggests that a small subunit of myosin must be a constituent of the clearing site. Several such small molecules have been found to be intimately related to the structure and function of myosin (Tsao, 1953; Locker, 1956; Kominz *et al.*, 1959; Gershman *et al.*, 1966; Locker and Hagyard, 1967; Weeds, 1967), and to be required for ADP binding to myosin (Dreizen and Gershman, 1969). The computer program has not been able to duplicate the curvature found in Figure 8.

Models Relating Turbidity and ATPase. (1) Both the ATPase and turbidity measurements on myofibrils and actomyosin are in general accord with the London–Steck (1969) model III of a basal and a metal-activated state. The ATPase activity of the basal state is that of myosin when $MgATP^{2-}$ is the modifier–reactant complex; its V_{max} is readily attained at moderate ATP concentration (Figure 2, curve 2). At low ATP concentration, neither the basal ATPase activity (Figure 2) nor the basal level of turbidity (Figure 7B) are dependent upon Ca^{2+} concentration. The metal-activated state is a hybrid one, with $MgATP^{2-}$ being the active substrate and Ca^{2+} the metal activator. Clearing (Figure 7A) and substrate inhibition (Figure 2) result when free ATP cooperatively binds to the clearing site and removes bound Ca^{2+}, causing dissociation of actomyosin (Maruyama and Gergely, 1962; Matsunaga and Noda, 1966).

These relations may be expressed in the form of a modified London–Steck model III

$$\begin{array}{ccccc} C + M^S & \overset{K_I}{\rightleftharpoons} & M_C{}^S & \overset{k'}{\longrightarrow} & M^S + \text{products} \\ \Big\downarrow\Big\uparrow A,S & & \Big\downarrow\Big\uparrow A,S & & \\ C + AM & \overset{K_{II}}{\rightleftharpoons} & AM_C & \overset{k''}{\longrightarrow} & AM + \text{products} \\ \Big\downarrow\Big\uparrow & & \Big\downarrow\Big\uparrow & & \\ C + (A)M & \overset{K_I}{\rightleftharpoons} & (A)M_C & \overset{k'}{\longrightarrow} & (A)M + \text{products} \end{array} \qquad (2)$$

Here C is $MgATP^{2-}$ and $M_{subscript}$ refers to the ATPase site. This model expresses the classical view that undissociated actomyosin constitutes the fully active enzyme. The independence of Ca^{2+} concentration at low ATP is here interpreted as due to ATP binding to a high affinity, low reactivity myosin site, with bound actin enzymatically inactive (A)M. An alternative explanation by Weber (1969) is that ATP must bind to the enzymatic sites on both heads of myosin (Slayter and Lowey, 1967) in a cooperative interaction before inhibition becomes possible. (2) When clearing occurs at intermediate levels of ATP, it may be accompanied by increased ATPase activity as indicated in Figure 6. This surprising correlation of actin dissociation with increased ATPase activity was first shown in H-meromyosin systems by Perry *et al.* (1963). As pointed out by Perry (1967), the classical view that only undissociated actomyosin is Mg^{2+}-activated may require revision.

Cyclic association–dissociation of the actin to myosin link offers an attractive alternative to the classical model. An equation for such a cyclic ATPase is

$$S + AM_C \rightleftharpoons AM_C{}^S \longrightarrow AM_{Mg}{}^S + \text{products} \rightleftharpoons A + M_{Mg}{}^S \rightleftharpoons AM_C \qquad (3)$$

In this equation, ATP bound to the clearing site participates in the cyclic ATPase. Such a role is supported by a number of experimental indications that clearing and ATPase activation are related. Reducing the ionic strength increases the apparent V_{max} and decreases the $pATP_{50}$ (Figure 11). The temperature dependence of clearing (Figure 12) and that of V_{max} (Levy *et al.*, 1959) have a similar break at 16–18°. The $\Delta H^{\ddagger}$ of ATPase activation is similar in magnitude and opposite in sign to the ΔH of clearing. Clearing has a large negative entropy, which could arise in part from the opening of bonds between actin and myosin, including hydrophobic bonds (Scheraga, 1963). In discussing the role of strain, distortion, and conformation change in catalysis, Jencks (1969) points

out that the potential binding energy of substrate or activator molecules may decrease the free energy of activation. If binding of ATP to the clearing site were coupled in this way to activation of the ATPase, a process leading to diminished binding energy should correspondingly increase the activation energy. The reduction in ΔH by about 20 kcal at low temperature (Table II) is indeed accompanied by an increased activation energy, found to go from about 12 to 25 kcal at 16° by Levy *et al.* (1959).

To re-form the actomyosin link after splitting ATP in a cyclic process, ATP must be released from the clearing site. Location of both the clearing and hydrolytic sites in a pocket of limited diffusion (Kominz and Yoshioka, 1969) could allow the hydrolytic site to generate an ATP concentration gradient affecting the clearing site. Such a local concentration gradient arises in the nonequilibrium analysis of muscle contraction (Caplan, 1966, 1968), and is indicated in data obtained from contractile muscle preparations (Bornhorst and Minardi, 1969).

Although the concentration of the unstable intermediate AM_C^S (calculated from eq 1 as previously described and employing a pK_{II}^d of 4.25 for the estimation of bound substrate) may exceed 10% of the total myosin, its pATP dependence cannot be correlated with experimental ATPase curves. Better correlation is obtained with the calculated values of AM_C, suggesting that if the cyclic model is valid, binding of ATP to the clearing site is the rate-limiting step.

Relation of Initial Clearing to Final Turbidity. It has been common practice to label any development of turbidity as "superprecipitation" and "contraction" synonymously, after the original example of Szent-Gyorgyi (1947). However at an early period Spicer (1952) had determined that superprecipitation is a two-stage reaction, an initial clear phase when the ATP concentration is high, followed by a second phase of turbidity development accompanied by precipitation or gelation upon depletion of ATP. Spicer (1951) suggested a relation between the second phase and postmortem rigor. Matsunaga and Noda (1966) were the first to show that a zone of ATP concentration exists at which intermediate states of clearing and flow birefringence can be found. The present work (Figures 9 and 10) extends the earlier findings by showing that the extent of final turbidity is proportional to the degree of initial clearing. It suggests that a conformational change has occurred during the initial plateau state (analogous to contraction) which is responsible for increased turbidity of the final state (analogous to rigor).

The molecular nature of the changes responsible for the final turbidity development are unknown; preliminary experiments suggest that binding of Ca^{2+} as well as release of ATP is involved. If clearing is produced in the presence of EGTA, the final turbidity is always less than if clearing is produced in the presence of traces of Ca^{2+}.

The present results support the conclusion of Levy and Fleisher (1965) that two or more molecules of ATP interacting at distinct sites are involved in superprecipitation. They suggest that the efficacy of a given quantity of ATP in the form of a few large additions rather than many small ones is because the former will produce greater transient clearing and consequently greater final turbidity. They similarly explain the increased turbidity produced by ATP at low temperatures as due to the increased efficiency of clearing at low temperatures.

References

Blum, J. J., and Morales, M. F. (1953), *Arch. Biochem. Biophys. 43*, 208.

Bornhorst, W. J., and Minardi, J. E. (1969), *Biophys. J. 9*, 654.

Caplan, S. R. (1966), *J. Theoret. Biol. 11*, 63.

Caplan, S. R. (1968), *Biophys. J. 8*, 1146.

Dreizen, P., and Gershman, L. C. (1969), *3rd Intern. Biophys. Congr.*, p 183.

Ebashi, S., and Ebashi, F. (1964), *J. Biochem. (Tokyo) 55*, 604.

Ebashi, S., and Endo, M. (1968), *in* Progress in Biophysics and Molecular Biology, Butler, J. A. V., and Huxley, H. E., Ed., Oxford, Pergamon, p 123.

Eisenberg, E., and Moos, C. (1965), *Arch. Biochem. Biophys. 110*, 568.

Evans, T. C., and Bowen, W. J. (1968), *Anal. Biochem. 25*, 136.

Finlayson, B., and Taylor, E. (1969), *Biochemistry 8*, 802.

Gershman, L. C., Dreizen, P., and Stracher, A. (1966), *Proc. Natl. Acad. Sci. U. S. 56*, 966.

Jencks, W. P. (1969), Catalysis in Chemistry and Enzymology, New York, N. Y., McGraw-Hill, Chapter 5.

Kiely, B., and Martonosi, A. (1968), *J. Biol. Chem. 243*, 2273.

Kominz, D. R. (1965), *Science 149*, 1374.

Kominz, D. R. (1966), *Arch. Biochem. Biophys. 115*, 583.

Kominz, D. R., Carroll, W. R., Smith, E. N., and Mitchell, E. R. (1959), *Arch. Biochem. Biophys. 79*, 191.

Kominz, D. R., and Yoshioka, K. (1969), *Arch. Biochem. Biophys. 129*, 609.

Kuby, S. A., and Noltmann, E. A. (1962), *Enzymes 6*, 515.

Levy, H. M., and Fleisher, M. (1965), *Biochim. Biophys. Acta 100*, 471, 491.

Levy, H. M., Sharon, N., and Koshland, D. E., Jr. (1959), *Proc. Natl. Acad. Sci. U. S. 45*, 785.

Lipmann, F., and Tuttle, L. C. (1945), *J. Biol. Chem. 195*, 21.

Locker, R. H. (1956), *Biochim. Biophys. Acta 20*, 514.

Locker, R. H., and Hagyard, C. J. (1967), *Arch. Biochem. Biophys. 120*, 454.

Loftfield, R. B., and Eigner, E. A. (1969), *Science 164*, 305.

London, W. P., and Steck, T. L. (1969), *Biochemistry 8*, 1767.

Maruyama, K., and Gergely, J. (1962), *J. Biol. Chem. 237*, 1095, 1100.

Maruyama, K., and Kominz, D. R. (1969), *J. Biochem. (Tokyo) 65*, 465.

Matsunaga, T., and Noda, H. (1966), *J. Biochem. (Tokyo) 60*, 674.

Morita, F. (1967), *J. Biol. Chem. 242*, 4501.

Morita, F. (1969), *Biochim. Biophys. Acta 172*, 319.

Nihei, T., and Tonomura, Y. (1959), *J. Biochem. (Tokyo) 46*, 305.

Perry, S. V. (1967), *in* Progress in Biophysics and Molecular Biology, Vol. 17, Butler, J. A. V., and Huxley, H. E., Ed., Oxford, Pergamon, p 325.

Perry, S. V., Cotterill, J., and Hayter, D. (1963), *Biochem. J. 100*, 289.

Perry, S. V., and Grey, T. C. (1956), *Biochem. J. 64*, 184.

Rose, I. A. (1962), *Enzymes 6*, 115.

Saroff, H. A. (1966), *in* Protides of the Biological Fluids, Vol. 14, Amsterdam, Elsevier, p 45.

Scheraga, H. A. (1963), *Proteins 1*, 477.

Sillen, L. B., and Martell, A. E. (1964), Stability Constants of Metal-Ion Complexes, London, The Chemical Society, p 651.

Slayter, H. S., and Lowey, S. (1967), *Proc. Natl. Acad. Sci. U. S. 58*, 1611.
Spicer, S. S. (1951), *J. Biol. Chem. 190*, 257.
Spicer, S. S. (1952), *J. Biol. Chem. 199*, 289.
Stowring, L., Bowen, W. J., Mattingly, P., and Morales, M. (1966), *Circ. Res. 19*, 496.
Szent-Gyorgyi, A. (1947), Chemistry of Muscular Contraction, New York, N. Y., Academic, p 31.
Tokiwa, T., and Tonomura, Y. (1965), *J. Biochem. (Tokyo) 57*, 616.
Tsao, T.-C. (1953), *Biochim. Biophys. Acta 11*, 368.
Weber, A. (1959), *J. Biol. Chem. 234*, 2764.
Weber, A. (1969), *J. Gen. Physiol. 53*, 780.
Weber, H. H., and Portzehl, H. (1952), *Advan. Protein Chem. 7*, 161.
Weeds, A. G. (1967), *Biochem. J. 105*, 25C.
Yagi, K., Nakata, T., and Sakakibara, I. (1965), *J. Biochem. (Tokyo) 58*, 236.

Studies on the Association of β-Chain Monomers of *Escherichia coli* Tryptophan Synthetase*

G. M. Hathaway and I. P. Crawford

ABSTRACT: Using the technique of sedimentation–diffusion equilibrium we have found measurable quantities of β-chain monomers, dimers, and possibly higher multimers in solutions of the B protein of *Escherichia coli* tryptophan synthetase. The multimers are in equilibrium; association constants for the monomer–dimer (K_2) and monomer–dimer–trimer (K_3) are estimated at 10.4 ± 0.5 and 1.4 ± 0.5 l./g, respectively, in 0.1 M potassium phosphate at pH 7.3. The association constant K_2 is markedly pH dependent over the range 6.5–9.5, and this change is reversible. K_2 is independent of temperature and ionic strength in the range 6–37.5° and up to $\Gamma/2 = 0.5$. We determined the distribution at sedimentation equilibrium of macromolecular species absorbing at 280, 335, and 415 nm. At 335 and 415 nm (absorption maxima due to the enzyme–cofactor complex) with low protein concentrations the solution appeared monodisperse at the dimer molecular weight of 89,000 daltons, suggesting that the monomer does not bind the cofactor. The monomer–dimer equilibrium is strongly affected by the presence or absence of cofactor, however.

Tryptophan synthetase from *Escherichia coli* is a heteropolymer separable into two components. Each of the separated components (termed A and B) will catalyze a partial reaction in the production of L-tryptophan from indoleglycerol phosphate and L-serine. It is well known that physical interaction between the A and B subunits takes place and that concomitant with this interaction a 10–100× increase is seen in the rate of each half-reaction (Crawford and Yanofsky, 1958). The A protein requires no cofactor, and contributes that portion of the active site of tryptophan synthetase involved in removal of the glycerol phosphate side chain from indoleglycerol phosphate. Primary amino acid sequence and molecular weight determinations have shown it to be a single polypeptide (α) of 28,700 daltons (Yanofsky *et al.*, 1967).

The B protein binds 2 moles of pyridoxal phosphate, and is involved in that part of the reaction attaching the alanyl moiety of L-serine to the indole portion of indoleglycerol phosphate. It is a homologous dimer (β_2) and although its primary sequence is not yet known, its molecular weight has been estimated to be 90,000 daltons (Hathaway *et al.*, 1969).

Previous investigations of the B protein in our laboratory showed it to be an associating system, with an association constant (K_2) for the monomer–dimer equilibrium not too large to preclude its measurement by presently available experimental techniques. This paper is concerned with the measurement of this type of interaction under various experimental conditions. Equations used in this work can be found in the Appendix.

Materials

Tris(hydroxymethyl)aminomethane, pyridoxal 5′-phosphate, and β-mercaptoethanol were purchased from the Sigma Chemical Co. Guanidine hydrochloride "ultra-pure" was obtained from Mann Research Laboratories. Doubly deionized or glass distilled, deionized water was used in all experiments. All chemicals were reagent grade and were used without further purification.

Methods

Analytical Gel Electrophoresis. Sodium dodecyl sulfate–acrylamide disc electrophoresis was performed using 7% gels essentially following the procedure of Shapiro *et al.*

* From the Department of Microbiology, Scripps Clinic and Research Foundation, La Jolla, California 92037. *Received November 20, 1969.* This work was supported by Grant GB6841 from the National Science Foundation, Grant AM 13224 from the National Institutes of Health, and funds from the Fleischmann Foundation.